Linear response results for phonons and electron–phonon coupling in hexagonal close packed

Sc-spin fluctuations, and implications for superconductivity

Linear response results for phonons and electron–phonon coupling in hexagonal close packed Sc-spin fluctuations, and implications for superconductivity

S K Bose

Physics Department, Brock University, St Catharines, ON, L2S 3A1, Canada

Abstract

We present a FP-LMTO (full-potential linear muffin-tin orbital) study of the variation in the electronic structure, phonon frequencies and electron–phonon coupling in hexagonal close packed (hcp) Sc under pressure. The electron–phonon coupling constant λ is found to increase steadily with pressure in the hcp phase, until the pressure reaches a value where the hcp phase becomes unstable. Linear response calculations for the normal pressure c/a ratio predict a phase change somewhere between calculated pressures of 22 and 30 GPa. The calculated frequencies for the equilibrium hcp lattice parameters are in good agreement with the inelastic neutron scattering results. There is a small upward shift in the Γ-point E_{2g} mode frequency under pressure, in qualitative agreement with the Raman spectroscopy study of Olijnyk *et al* (2006 *J. Phys.: Condens. Matter* **18** 10971). From the measured value of the electronic specific heat constant and the calculated values of the Fermi level density of states and electron–phonon coupling constant, we conclude that the electron–paramagnon coupling constant in hcp Sc should be comparable to the electron–phonon coupling constant. This indicates that the spin fluctuation effects are strong enough to suppress superconductivity completely in hcp Sc. We argue that spin fluctuations should be reduced by a factor of two or more in the high pressure Sc-II phase. On the basis of estimates of the electron–paramagnon coupling constants and the calculated or estimated electron–phonon coupling constants, we argue that the hcp phase may become superconducting with a very low transition temperature immediately prior to the transition to the Sc-II phase and that the Sc-II phase should indeed be superconducting. The electronic, electron–phonon and spin fluctuation properties of hcp Sc under pressure are compared with those of the high pressure hcp phase of Fe, which was reported to be superconducting a few years back.

1. Introduction

This work was motivated by a recent work of Hamlin and Schilling [1], who reported the measurement of the superconducting transition temperature T_c in Sc as a function of pressure. Superconductivity in Sc is induced under pressure, with T_c increasing monotonically to 8.2 K at 74.2 GPa. Hamlin and Schilling [1] report measurements of T_c between $\sim$55 GPa ($T_c \sim 5$ K) and 74.2 GPa ($T_c = 8.2$ K). The normal pressure phase of Sc is hcp and it is known to undergo several changes in its crystal structure as a function of pressure, the first such transition known to be occurring around 22–23 GPa [3–5] from

hcp (Sc-I) to a complicated structure, referred to as Sc-II. To date the normal and low pressure hcp phase is known to be non-superconducting. Earlier work by Wittig *et al* [2] showed that superconductivity is possibly induced in the hcp phase at high pressure around 20 GPa, immediately before it enters the complex Sc-II phase. T_c in the hcp phase was estimated to be less than 0.1 K.

Ab initio theoretical studies of superconductivity in Sc as a function of pressure is rendered difficult by the fact that the superconducting Sc-II phase is not only complex, but also that its exact structure still remains open to investigation and refinement [3–5]. Ormeci *et al* [22] have studied the electronic

structure of the Sc-II phase proposed by Fujihisa *et al* [3] and McMahon *et al* [5] and produced results suggesting that the structure proposed by McMahon *et al* might provide a better representation of the Sc-II phase. Both of these proposed structures are composite incommensurate structures, consisting of host and guest substructures.

　　In this communication we present *ab initio* calculations of the electronic structure, elastic properties, phonons and electron–phonon coupling in the low pressure hcp phase of Sc. The purpose is to shed some light on why hcp Sc is not superconducting, while the substance might become superconducting under pressure. Several scenarios are possible. It might be that the electron–phonon coupling in the hcp phase is small, making superconductivity unlikely in this phase. This coupling may increase with pressure, but still remain too small for superconductivity to appear over the entire pressure range for which the hcp phase is stable. Another possibility is that the electron–phonon coupling is strong enough to support superconductivity in the hcp phase. In this latter scenario one needs to explore why superconductivity is suppressed in the hcp phase and appears only in the high pressure Sc-II phase. Calculations of the phonon frequencies as a function of pressure should also show softening of certain modes leading to the instability of the hcp phase at high pressure.

　　We use the full-potential linear muffin-tin orbital (FP-LMTO) method [6] to study the electronic structure and the linear response scheme developed by Savrasov [7, 8] to compute the phonon frequencies, the Eliashberg spectral function and the electron–phonon coupling constant λ as a function of volume in hcp Sc. For the sake of simplicity and convenience in the calculation, the c/a ratio is kept fixed at the normal pressure value [9]. This restriction of the c/a ratio being kept fixed at the normal pressure value should not be of any concern from the viewpoint of the main results and conclusions of this work. This will become clear from the discussion in the following sections.

　　Sc is the lightest of the 3d-transition metals. It would be of interest to see how the electron–phonon coupling in hcp Sc compares with that of the late transition metal hcp Fe, which was reported to be superconducting by Shimizu *et al* [10] (see also [11]) a few years back. The hcp phase is the stable phase of Fe at pressures ∼10 GPa and higher. Bose *et al* [12] reported FP-LMTO linear response results for hcp Fe. They showed, in agreement with earlier LAPW(linear augmented plane-wave)-based rigid muffin-tin (RMT) results of Mazin and co-workers [13], that not only should hcp Fe be superconducting, but also conventional (electron–phonon) s-wave superconductivity in hcp Fe should persist up to a much higher pressure than what is found in the experiments. Both ferromagnetic and antiferromagnetic spin fluctuation effects were considered in the works of Bose *et al* [12] and Mazin *et al* [13]. The conclusion was that such spin fluctuation effects in hcp Fe could lower T_c somewhat, but could not account for the rapid disappearance of T_c with increasing pressure, as observed by Shimizu *et al* [10]. Nontrivial differences between the electronic structures of Fe and Sc, due in particular to the large difference in the number of d-electrons, cause
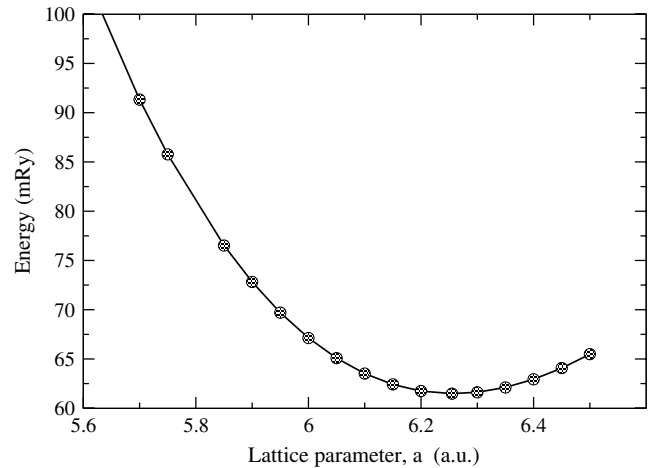

Figure 1. FP-LMTO total energy per atom versus the lattice parameter in hcp Sc for the $c/a = 1.592$, valid for the normal pressure values: $a = 3.31$ Å, $c = 5.27$ Å [9]. For convenience in plotting, a constant value of -1529.0 Ryd from the total energy per atom has been subtracted.

significant differences in their elastic as well as electron–phonon scattering properties, which should have opposite effects on the overall electron–phonon coupling constant.

　　Ormeci *et al* [22] have used crystalline approximants of the incommensurate structures proposed by Fujihisa *et al* [3] and McMahon *et al* [5] in studying the electronic structure of the Sc-II phase. The unit cells of these approximants contain 22 atoms for the model proposed by Fujihisa *et al* [3] and 42 atoms for the model suggested by McMahon *et al* [5]. Because of the high computational demand due to the large number of atoms in the unit cells of these approximants, we are unable to extend the linear response calculations of phonons and electron–phonon coupling to the Sc-II phase.

2. Electronic structure

FP-LMTO results of total energy as a function of the lattice parameter in hcp Sc is shown in figure 1. The c/a ratio was kept fixed at the normal pressure value [9]. As in the earlier calculation for hcp Fe [12], the generalized gradient approximation of Perdew and Wang (GGA1) [14] for the exchange–correlation potential was used. The electronic structure was computed using a two-κ spd LMTO basis for the valence band. 3s- and 3p-semi-core states were treated as valence states in separate energy windows. The charge densities and potentials were represented by spherical harmonics with $l \leqslant 6$ inside the non-overlapping MT spheres and by plane waves with energies $\leqslant 48$–70 Ryd, depending on the lattice parameter, in the interstitial region. Brillouin zone (BZ) integrations were performed with the full-cell tetrahedron method [15], using 1200 **k**-points in the irreducible zone. The pressure and bulk modulus calculated from this energy-volume curve, using the generalized Birch–Murnaghan equation of state [16, 17], are shown in table 1. Note that the minimum energy occurs almost exactly at the normal pressure lattice parameter of 6.255 au. The calculated bulk modulus of
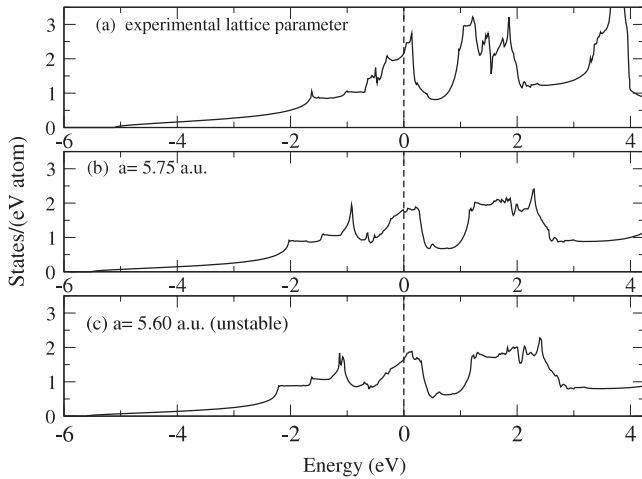
Figure 2. FP-LMTO DOSs for three lattice parameters of hcp Sc:
(a) normal pressure values [9]: $a = 6.255$ au, $c/a = 1.592$,
(b) $a = 5.75$ au and (c) $a = 5.60$ au; c/a ratio for (b) and (c) is the
same as in (a). It appears that as the Fermi level moves from the
shallow valley region between two small peaks (a) to a shoulder (c),
the hcp structure becomes unstable.

Table 1. FP-LMTO results for hcp Sc for the normal pressure c/a
ratio, 1.592. a = lattice parameter (au), V_0 = volume per atom (au),
P = pressure (GPa), B = bulk modulus (GPa), $N(0)$ = DOS at the
Fermi level (states/(Ryd cell)).

a	6.255	6.15	6.05	5.95	5.85	5.75
V_0	168.72	160.37	152.67	145.22	138.02	131.07
P	−0.084	3.21	6.85	11.22	16.20	22.28
B	56.2	67.2	79.6	93.0	108	125
$N(0)$	58.06	54.82	51.59	49.07	47.27	47.71

56 GPa at this [9] equilibrium lattice parameter is somewhat
higher than the experimental value, 43.5 GPa. One interesting
observation is that the lattice parameter 5.75 au, or the volume
per atom $V_0 = 131$ au, corresponds to a pressure of 22 GPa.
This is the pressure at which the hcp Sc-I phase becomes
unstable against the formation of a complicated structure
known as the Sc-II phase [3–5]. As will be discussed later,
the linear response results show that the phonon frequencies
calculated for lattice parameter $a = 5.6$ au are imaginary.
Thus, for the normal pressure c/a ratio, the hcp structure
becomes unstable at some lattice parameters between 5.75 and
5.6 au. The calculated pressure at 5.6 au is ∼30 GPa. Given the
uncertainties in the pressure calculation, this result is in good
agreement with the experimental observation of a phase change
in Sc at 22–23 GPa. Additional linear response calculations to
better locate the phase change were not done.

The FP-LMTO DOS calculated for three lattice parame-
ters are shown in figure 2. Panel (a) shows the DOS for the
experimental normal pressure lattice parameters: $a = 3.31$ Å,
$c = 5.27$ Å [9]. Panels (b) and (c) show the DOSs for the lat-
tice parameters 5.75 and 5.60 au, respectively, with the same
c/a ratio as in (a). For the equilibrium lattice parameters (panel
(a)), the Fermi level falls in a shallow valley between two small
peaks. With increasing pressure, the bands broaden, flattening
these peaks and the valley region (panel (b)). It appears that as

Table 2. LMTO-ASA results for (approximate) s-, p-, d- and
f-orbital resolved charges: n_s, n_p, n_d, n_f and the corresponding Fermi
level DOSs: N_s, N_p, N_d, N_f. $n' = \frac{n_d + n_f}{n_s + n_p}$, $n^- = (n_d + n_f) - (n_s + n_p)$
and $N' = \frac{N_d + N_f}{N_s + N_p}$ are presented to reveal the trends in the inter-orbital
charge transfer and the redistribution of the orbital-resolved DOSs as
a function of volume per atom. $N(0)$ is the total DOS at the Fermi
level. All DOSs are in units of states/(Ryd cell). a = lattice
parameter (au).

a	6.255	6.15	6.05	5.95	5.85	5.75
n_s	0.730	0.720	0.714	0.704	0.695	0.685
n_p	0.690	0.677	0.662	0.645	0.626	0.603
n_d	1.545	1.567	1.589	1.614	1.641	1.672
n_f	0.031	0.033	0.034	0.036	0.037	0.039
n^-	0.156	0.203	0.247	0.301	0.357	0.423
n'	1.11	1.15	1.18	1.22	1.27	1.33
$N(0)$	57.89	54.78	53.03	51.60	50.16	53.34
$N_s(0)$	0.941	0.946	0.964	0.982	1.020	1.226
$N_p(0)$	14.836	13.729	12.889	12.257	11.914	13.558
$N_d(0)$	40.789	39.110	37.887	37.080	36.444	37.222
$N_f(0)$	1.326	1.301	1.287	1.280	1.280	1.335
N'	2.67	2.75	2.83	2.90	2.92	2.60

this region around the Fermi level changes to a shoulder (panel
(c)), the hcp phase becomes unstable.

Hamlin and Schilling [1] discuss the importance of the
role of s → d charge transfer in the variation of electron–
phonon coupling and the changes in the crystal structure under
pressure. Pettifor [18] has discussed the variation of the d-band
occupancy under pressure of 4d-transition metals, showing that
the increase in the d-electron occupancy of the early transition
metals under pressure is rapid. Duthie and Pettifor [19]
used a s–d band model to discuss the correlation between
the d-band occupancy and the crystal structures in rare-earths.
They showed that d-electron concentration n_d increases under
pressure and a sequence of crystal structure changes takes place
as n_d changes from 1.5 to 2.5. With increasing pressure, the
volume available to the electrons outside the ion cores
diminishes rapidly. As a result, simple metals like Li and Na
are known to become non-free-electron-like under pressure and
Cs is known to become a transition metal as the 5d-band begins
to fill due to s → d charge transfer (see references in [1]). In
any electronic structure calculation the numbers of s-, p- and
d- electrons are essentially functions of the basis set used, if
such a division is at all possible for the method used. It is
easier to keep track of s → d charge transfer in LMTO-ASA
(atomic sphere approximation) [20], where the basis consists of
muffin-tin orbitals only, rather than in FP-LMTO. In table 2 we
present the orbital- or partial wave channel-resolved electron
numbers as a function of the lattice parameter, as obtained by
the LMTO-ASA method[1]. The results presented were obtained
by using the exchange correlation potential of Perdew and
Wang [21] in the local density approximation. Checks for a
couple of lattice parameters using GGA1 [14] had revealed
similar results. The decrease in n_s and the increase in n_d
are monotonic as a function of decreasing lattice parameters.

[1] Inside each muffin-tin (atomic) sphere there is a small contribution from
the tails of orbitals centered about the surrounding spheres. This may cause
a disproportionate increase in the high l-components, particularly $l = 3$. The
increase in the n_f with decreasing volume may be partly due to this effect.

Table 3. Hopfield parameters from the linear response calculation η and the rigid muffin-tin (atomic sphere) approximation η (RMT/RAS), the Fermi surface average of the square of the electron–phonon matrix element $\langle I^2 \rangle$ and $\langle I^2 \rangle$ (RMT/RAS) from the linear response and the RMT results, respectively; logarithmic average phonon frequencies ω_{ln}; maximum phonon frequencies ω_m, average phonon frequencies $\bar{\omega} = \langle \omega \rangle$ and $\tilde{\omega} = \langle \omega^2 \rangle^{1/2}$; the Γ-point E_{2g} mode frequency $\omega(E_{2g})$; Coulomb pseudopotentials for Eliashberg equation ($\mu^*(\omega_c)$) and McMillan formula (μ^*_{ln}); electron–phonon coupling parameters λ_{ph}; calculated critical temperatures (T_c^{calc}) from the solution of the Eliashberg equations (2) and the critical temperatures from the McMillan formula (9) (T_c^{McM}) for various lattice parameters a.

a	a_B	6.255	6.15	6.05	5.85	5.75
η	Ryd/bohr^2	0.0381	0.0433	0.0519	0.0666	0.0771
$\langle I^2 \rangle$	(Ryd/bohr)^2	0.0026	0.0031	0.0040	0.0056	0.0065
η (RMT/RAS)	Ryd/bohr^2	0.0439	0.0509	0.0591	0.0826	0.1077
$\langle I^2 \rangle$ (RMT/RAS)	(Ryd/bohr)^2	0.0030	0.0037	0.0045	0.0065	0.0081
	K	160.4	195.0	198.1	195.4	177.7
ω_{ln}	cm^{-1}	111.5	135.5	137.7	135.8	123.5
ω_m	cm^{-1}	214.5	230.4	246.9	279.6	294.7
$\omega(E_{2g})$	cm^{-1}	130.5	134.95	133.4	136.14	135.0
$\bar{\omega}$	cm^{-1}	122.4	142.3	145.1	145.6	135.3
$\tilde{\omega}$	cm^{-1}	131.5	148.6	152.3	155.8	148.1
$\mu^*(\omega_c)$		0.253	0.256	0.260	0.266	0.269
$\mu^*(\omega_{\mathrm{ln}})$		0.160	0.161	0.163	0.165	0.166
λ_{ph}		0.639	0.576	0.657	0.807	1.033
T_c^{McM}	K	2.34	1.66	2.96	5.66	9.18
T_c^{calc}	K	2.17	1.75	3.13	6.00	9.64

In fact, charge transfer takes place from the extended s- and p-orbitals to the less extended or localized d- and f-orbitals. Of particular interest are n' and n^-, defined as $n' = \frac{n_d + n_f}{n_s + n_p}$ and $n^- = (n_d + n_f) - (n_s + n_p)$, quantifying the transfer of electrons from the delocalized to the localized channels. At normal pressure the electrons are divided almost equally between the localized and delocalized channel ($n^- = 0.15$). With increasing pressure the electrons more and more occupy the localized orbitals.

As the pressure increases different partial bands broaden at different rates. In table 2 we also show the changes in partial or angular momentum-resolved DOSs at the Fermi level. The ratio of the localized orbital DOSs ($N_d(0) + N_f(0)$) to the delocalized orbital DOSs ($N_s(0) + N_p(0)$) seem to increase steadily under pressure, except for the lowest lattice parameter shown. The decrease in N' for the lattice parameter 5.75 au could be specific to LMTO-ASA, as the somewhat large change in $N(0)$ between the lattice parameters 5.85 and 5.75 au is not observed in the FP-LMTO results (table 1).

Ormeci et al [22] have calculated the partial charges in the high pressure Sc-II phase. They use the full-potential local-orbital (FPLO) method of Koepernik and Eschrig [23] with an spd-basis. At ambient pressure, in the hcp structure, their nl-projected charges for the 4s, 4p, and 3d channels are 0.70, 0.59 and 1.70, respectively. In the Sc-II phase at about two thirds of the ambient pressure volume per atom, these numbers become 0.54–0.65, 0.27–0.51, and 1.92–2.05, respectively. Their calculations also suggest that a complete s → d charge transfer would require pressures in excess of 240 GPa.

3. Phonons and electron–phonon coupling

The FP-LMTO linear response results for phonons and electron–phonon coupling are summarized in table 3. The dynamical matrix was generated for 32 phonon wavevectors in the irreducible BZ, corresponding to a mesh of (7, 7, 7)

reciprocal lattice divisions. The BZ sums for the dynamical and electron–phonon (Hopfield) matrices was done for a (28, 28, 28) mesh, resulting in 1200 wavevectors in the IBZ. These choices were based on extensive tests performed by Savrasov and Savrasov [7, 8] in their study of the phonons and electron–phonon coupling in elemental metals and alloys. Phonon density of states $F(\omega)$, Eliashberg spectral function $\alpha^2 F(\omega)$ and the function $\alpha^2(\omega) = \alpha^2 F(\omega)/F(\omega)$ are shown in figure 3 for three different lattice parameters with the c/a ratio fixed at the normal pressure value.

The calculated phonon frequencies appear to be in reasonably good agreement with the inelastic neutron scattering (INS) results [24, 25]. For the normal pressure lattice parameter (6.255 au), the calculated longitudinal and transverse optic (LO and TO) mode frequencies at the Γ-point are 6.273 THz (209 cm^{-1}) and 3.912 THz (130.5 cm^{-1}), respectively. These compare well with the inelastic neutron scattering results of Wakabayashi et al [24]: 6.91 and 4.04 THz for the LO and TO modes, respectively. The recent Raman spectroscopy study of Olijnyk et al [26] puts the TO mode (E_{2g}) frequency at a somewhat higher value of 139 cm^{-1}. On the whole, the calculated frequencies are a bit lower than the INS results of Wakabayashi et al [24]. These authors have analyzed the INS results in terms of a sixth-neighbor modified axially symmetric force constant model and produce a frequency distribution, which reveals a maximum frequency of about 7.25 THz or 241.8 cm^{-1}, approximately 10% higher than the maximum calculated frequency 215 cm^{-1} (table 3) in this work. The shape of the frequency distribution agrees in general with the phonon DOS $F(\omega)$ shown in figure 3, except for the relative heights of some of the low frequency peaks.

The Raman spectroscopy work by Olijnyk et al [26] shows a shift of the E_{2g} frequency under pressure from 139 cm^{-1} to about 150 cm^{-1} at 18.8 GPa. The calculated Γ-point TO mode frequency increases from 130.5 cm^{-1} at the normal pressure lattice parameter ($a = 6.255$ au) to 135.1 cm^{-1} at
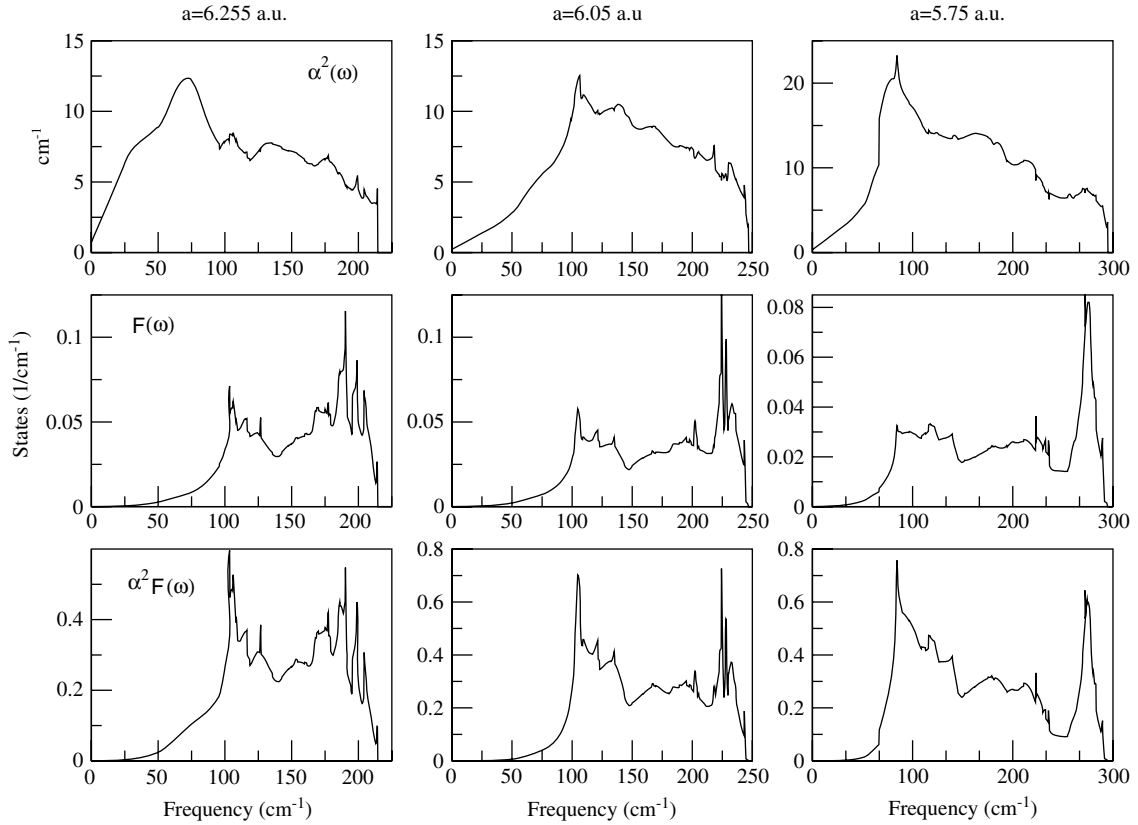
Figure 3. Phonon density of states $F(\omega)$, the Eliashberg spectral function $\alpha^2 F(\omega)$ and the function $\alpha^2(\omega)$, defined as the ratio $\alpha^2 F(\omega)/F(\omega)$, for three lattice parameters $a = 6.255$ (experimental normal pressure value), 6.05, and 5.75 au, with c/a ratio fixed at the normal pressure value.

$a = 5.75$ au, i.e., the increase is much more subdued. In table 3 we have presented the calculated E_{2g} frequency for various lattice parameters. Although the variation may seem non-monotonic, the differences are very much within the error bars of the calculation. What can perhaps be concluded is that there is no phonon softening and most probably this frequency does increase by approximately 5 cm^{-1}. This is about 45–50% of the observed shift. Note that calculations for the stable hcp phase for a lattice parameter between 5.75 and 5.6 au might reveal a higher shift. The discrepancy between the calculated and the observed shift could be partly due to the possible variation in the c/a ratio under pressure, which has not been considered in the calculation. Olijnyk *et al* [26] have analyzed the shift in the E_{2g} frequency in terms of the relation

$$\mu_{E_{2g}} = \frac{1}{2\pi}\left(\frac{4\sqrt{3}a^2 C_{44}}{mc}\right)^{1/2}, \tag{1}$$

where m is the atomic mass and C_{44} is the elastic shear modulus. They relate their result to the behavior of the shear modulus at the transition. The possible variation of the c/a ratio with pressure should be factored in this discussion. The coarse wavevector mesh used for the phonon frequency calculation prevents us from using the slope of the phonon dispersion curves or the long wavelength method to compute the elastic constants. *Ab initio* calculation of the elastic constants, including C_{44}, via long wavelength and

homogeneous deformation methods using energy-minimized c/a ratios will be the subject of a separate publication.

It is noteworthy that both calculation and the Raman study show a positive shift of the E_{2g} frequency, in contrast to the behavior in Y and the regular Lanthanides, where a softening of the E_{2g} mode under pressure is associated with the transition to the high pressure Sm-type structure [27, 28]. Incidentally, in our linear response calculation, as the lattice parameter is lowered to 5.6 au where the instability of the hcp phase is manifest via the appearance of some imaginary frequencies, the E_{2g} mode frequency stays real and has a lower value 124 cm^{-1}. At a lattice parameter of 5.2 au, this frequency, along with many others, are imaginary.

Broadening of the phonon bands and the increase in the maximum phonon frequencies with pressure is apparent in figure 3. Maximum phonon frequency increases from 215 to 295 cm^{-1}, as the lattice parameter changes from the normal pressure value to 5.75 au, where the estimated pressure (table 1) is 22–23 GPa. Note that with increasing pressure, initial increases in $\bar{\omega}$, $\tilde{\omega}$ and ω_{ln} are followed by a decrease, revealing phonon softening. At normal pressure, the shape of the $\alpha^2 F(\omega)$ function follows that of the phonon DOS $F(\omega)$. With increasing pressure, differences between the shape of the two functions appear due to increased contribution from low frequency phonons, a consequence of phonon softening. There is a feed-back effect: electron–phonon coupling leads to both phonon linewidth and renormalization of the phonon

frequency, and the latter, in turn, affects the coupling constant. Unfortunately, the 7, 7, 7 division of the BZ misses most of the symmetry points. However, it appears that there are several regions of the wavevector space that show large mode coupling. Linear response calculations for the lattice parameter 5.6 au show that the phonon frequency at the wavevector closest to the L-point for the 7, 7, 7 division becomes imaginary first. For the lattice parameter 5.75 au, this wavevector has a very large mode coupling constant. In table 3, it is clear that general phonon softening starts as the lattice parameter increases beyond 6.05 au (as seen from ω_{ln}) or 5.85 au (as seen from $\bar{\omega}$ and $\tilde{\omega}$), while the E_{2g} mode continues to stiffen and the maximum phonon frequency continues to increase.

The electron–phonon coupling parameter λ_{ph} is a combination of an electronic parameter (Hopfield parameter) $\eta = \langle I^2 \rangle N(0)$ ($N(0)$ being the Fermi level DOS for one type of spin) and the mean square phonon frequency $\langle \omega^2 \rangle$: $\lambda_{\mathrm{ph}} = \eta / m \langle \omega^2 \rangle$. $\langle I^2 \rangle$ is the Fermi surface average of the square of the electron–phonon matrix element. The electronic and phonon-related parameters act in opposite directions in affecting the coupling constant: λ is enhanced by having higher $\langle I^2 \rangle$ at lower frequency. As the Hopfield parameter for transition metals has often been calculated using the rigid muffin-tin approximation of Gaspari and Gyorffy [30], in table 3 we have compared the values obtained via the FP-LMTO linear response method (η) and those obtained by using the RMT scheme implemented within the LMTO-ASA method [31, 32], known as the rigid atomic sphere (RAS) method. The latter values, labeled as $\eta(\mathrm{RMT/RAS})$, are in general agreement with the FP-LMTO results, but are somewhat overestimated, with the level of the overestimation increasing with pressure. This is in contrast with the results for the late transition metal hcp Fe, where RAS was shown to consistently underestimate the Hopfield parameter, with the level of the underestimation increasing with pressure [12]. The values of the Fermi surface averaged electron–phonon matrix element $\langle I^2 \rangle$, obtained from the linear response calculation and by using the RMT approximation, are also shown in table 3.

4. Superconductivity in hcp Sc, based purely on electron–phonon coupling

Since *ab initio* results of the electron–phonon coupling in hcp Sc have not been reported in the literature, it would be of some interest to derive values of the superconducting transition temperature T_c based on the present calculations. Indeed, the values of the coupling constant λ_{ph} listed in table 3 suggest that T_c could be high enough to be experimentally observable. The superconducting transition temperature can be obtained by solving the linearized isotropic Eliashberg equation at T_c (see, e.g., [29]):

$$Z(i\omega_{\mathrm{n}}) = 1 + \frac{\pi T_c}{\omega_{\mathrm{n}}} \sum_{n'} W_+(n-n')\,\mathrm{sgn}(\omega_{n'}),$$

$$Z(i\omega_{\mathrm{n}})\Delta(i\omega_{\mathrm{n}}) = \pi T_c \sum_{n'}^{|\omega_{\mathrm{n}}| \ll \omega_c} W_-(n-n')\frac{\Delta(i\omega_{n'})}{|\omega_{n'}|}, \tag{2}$$

where $\omega_{\mathrm{n}} = \pi T_c(2n+1)$ is a Matsubara frequency, $\Delta(i\omega_{\mathrm{n}})$ is an order parameter and $Z(i\omega_{\mathrm{n}})$ is a renormalization factor. Interactions W_+ and W_- contain a phonon contribution λ_{ph}, a contribution from spin fluctuations λ_{sf}, and effects of scattering from impurities. With scattering rates $\gamma_m = \frac{1}{2\tau_m}$ and $\gamma_{nm} = \frac{1}{2\tau_{\mathrm{nm}}}$ referring to magnetic and nonmagnetic impurities, respectively, the expressions for the interaction terms are:

$$W_+(n-n') = \lambda_{\mathrm{ph}}(n-n') + \lambda_{\mathrm{sf}}(n-n') + \delta_{nn'}(\gamma_{\mathrm{nm}} + \gamma_{\mathrm{m}}), \tag{3}$$

and

$$W_-(n-n') = \lambda_{\mathrm{ph}}(n-n') - \lambda_{\mathrm{sf}}(n-n') - \mu^*(\omega_c) + \delta_{nn'}(\gamma_{\mathrm{nm}} - \gamma_{\mathrm{m}}). \tag{4}$$

The phonon contribution is given by

$$\lambda_{\mathrm{ph}}(n-n') = 2\int_0^\infty \frac{\mathrm{d}\omega\,\omega\alpha^2(\omega)F(\omega)}{(\omega_{\mathrm{n}} - \omega_{\mathrm{n'}})^2 + \omega^2}, \tag{5}$$

where $\alpha^2(\omega)F(\omega)$ is the Eliashberg spectral function, defined as

$$\alpha^2 F(\omega) = \frac{1}{N(0)} \sum_{\mathbf{k},\mathbf{k'},ij,\nu} |g_{\mathbf{k},\mathbf{k'}}^{ij,\nu}|^2 \delta(\varepsilon_{\mathbf{k}}^i)\delta(\varepsilon_{\mathbf{k'}}^j)\delta(\omega - \omega_{\mathbf{k}-\mathbf{k'}}^\nu). \tag{6}$$

Here, $g_{\mathbf{k},\mathbf{k'}}^{ij,\nu}$ is the electron–phonon matrix element, with ν being the phonon polarization index and $\mathbf{k}, \mathbf{k'}$ representing electron wavevectors with band indices i, and j, respectively. $\lambda_{\mathrm{ph}}(0) = \lambda_{\mathrm{ph}}$ is the electron–phonon coupling parameter, the values of which are given in table 3. The contribution connected with spin fluctuation can be written as

$$\lambda_{\mathrm{sf}}(n-n') = \int_0^\infty \frac{\mathrm{d}\omega^2\,P(\omega)}{(\omega_{\mathrm{n}} - \omega'_{\mathrm{n}})^2 + \omega^2}, \tag{7}$$

where $P(\omega)$ is the spectral function of spin fluctuations, related to the imaginary part of the transversal spin susceptibility $\chi_\pm(\omega)$ as

$$P(\omega) = -\frac{1}{\pi}\left\langle |g_{\mathbf{k}\mathbf{k'}}|^2 \,\mathrm{Im}\chi_\pm(\mathbf{k},\mathbf{k'},\omega)\right\rangle_{\mathrm{FS}},$$

where $\langle\rangle_{\mathrm{FS}}$ denotes the Fermi surface average. $\lambda_{\mathrm{sf}} = \lambda_{\mathrm{sf}}(0)$ is often referred to as the electron-paramagnon coupling constant. In equation (4), $\mu^*(\omega_c)$ is the screened Coulomb interaction,

$$\mu^*(\omega_c) = \frac{\mu}{1 + \mu \ln(E/\omega_c)}, \tag{8}$$

with $\mu = \langle N(0)V_c\rangle_{\mathrm{FS}}$ being the Fermi surface average of the Coulomb interaction. E is a characteristic electron energy, usually chosen as the Fermi energy E_F and ω_c is a cut-off frequency, usually chosen ten times the maximum phonon frequency: $\omega_c \simeq 10\omega_{\mathrm{ph}}^{\mathrm{max}}$.

For a start, we ignore all consideration of spin fluctuations and impurity scattering and solve the Eliashberg equation with only the electron–phonon term and the Coulomb pseudopotential $\mu^*(\omega_c)$. As is often done, we assume that a reasonable value for μ is ~1.0, and from the calculated Fermi energies E_F we obtain μ^* for all volumes, with the cut-off

frequency ω_c assumed to be ten times the maximum phonon frequency. The values are listed in table 3. As shown in this table, the superconducting transition temperature in hcp Sc based on consideration of electron–phonon coupling alone can be significant, increasing monotonically with pressure from 2 K to $\sim$10 K until the instability of the hcp phase sets in. Interestingly, the T_c values reported by Hamlin and Schilling [1] for the high pressure Sc-II phase fall in this range, while no superconducting behavior has been observed in the hcp phase.

For pedagogical reasons, we have listed in table 3 the values of T_c obtained by using the Allen-Dynes form [29] of the McMillan expression:

$$T_c = \frac{\omega_{\ln}}{1.2} \exp\left\{ -\frac{1.04\left(1 + \lambda_{\mathrm{ph}}\right)}{\lambda - \mu^*(1 + 0.62\lambda_{\mathrm{ph}})} \right\}, \qquad (9)$$

where $\omega_{\ln}$ is the logarithmically averaged phonon frequency [29], obtained from our linear response calculations and reported in table 3. Note that the Coulomb pseudopotential μ^* appearing in the McMillan equation above is related to $\mu^*(\omega_c)$ appearing in the Eliashberg equation via [29]

$$\mu^* = \mu^*(\omega_{\ln}) = \frac{\mu^*(\omega_c)}{(1 + \mu^*(\omega_c)\ln(\omega_c/\omega_m))}. \qquad (10)$$

Our results are computed with $\omega_c/\omega_m = 10$. The T_c values obtained by solving the Eliashberg equations and those from the McMillan expression equation (9) show excellent agreement. Earlier, calculations for hcp Fe [12] had shown the McMillan expression to overestimate T_c with respect to the results from the Eliashberg equation, while for fcc and bct boron an opposite trend was revealed [33].

5. Spin fluctuation effects

5.1. hcp Sc at normal pressure

Faced with the results of the previous section, one needs to produce convincing arguments as to why hcp Sc is not superconducting despite sufficiently strong electron–phonon coupling. A mechanism that is known to cause suppression of superconductivity is spin fluctuations, which is often quoted as the reason why fcc Pd is not superconducting [34]. It is argued that the high value of $N(0)$ in fcc Pd leads to considerable Stoner enhancement of paramagnetic spin susceptibility, making it a borderline ferromagnetic material, and spin fluctuations tending to ferromagnetic alignment of spins lead to the breaking of the Cooper pairs. That such a mechanism is operative in hcp Sc as well is highly probable and has been discussed in the literature on a few occasions [35, 36]. Jensen and Maita [37] argue that the spin fluctuation effects are responsible for the rapid depression of T_c in the Zr–Sc alloy system, as Sc is added. *Ab initio* calculations of the spin susceptibility of hcp Sc at equilibrium volume based on the spin-density functional theory by MacDonald *et al* [38] yield an exchange–correlation enhancement factor of 4.03 over the band value and 17.2 over the free-electron value at the same average electron density as in hcp Sc. An earlier calculation by

Das [36] puts the Stoner enhancement factor at 4.6 (over the band value). The value calculated for fcc Pd by Janak [39] is 4.46. This shows that the spin fluctuations in hcp Sc should be as strong as in fcc Pd.

For a proper theoretical treatment of the spin fluctuation effects one needs to compute $\lambda_{\mathrm{sf}}(n - n')$ from the spin susceptibility function given by equation (7). However, it is important to note that such treatments tacitly assume a Migdal-like theorem being applicable to spin fluctuations. The Eliashberg equations (equation (2)) are based on the assumption that the maximum or the cut-off energy of spin fluctuation is much smaller than the characteristic electronic energy, e.g. the Fermi level. A somewhat qualitative treatment of spin fluctuations can be based on estimating $\lambda_{\mathrm{sf}} = \lambda_{\mathrm{sf}}(0)$ from experiments. Both electron–phonon and the electron-paramagnon interactions contribute to the electronic specific heat. In an independent one-electron picture this is interpreted as the electronic mass enhancement or equivalently, enhancement of the density of states over the bare value $N(0)$. The latter is the value given by calculations, where these interactions are not included in the one-electron Hamiltonian. Thus, a reliable estimate of the electron-paramagnon coupling constant λ_{sf} can be obtained from the measured value of the temperature co-efficient of the electronic specific heat γ, and the calculated values of the bare electron density of states and the electron–phonon coupling constant λ_{ph}:

$$\gamma = \frac{\pi^2}{3} k_B^2 N^*(0) \qquad (11)$$

$$N^*(0) = N(0)(1 + \lambda_{\mathrm{eff}}) \qquad (12)$$

$$\lambda_{\mathrm{eff}} = \lambda_{\mathrm{ph}} + \lambda_{\mathrm{sf}}. \qquad (13)$$

Here, γ and $N(0)$ refer to the values per atom. The Coulomb interactions are included in an average sense in the density functional calculations of $N(0)$, and have therefore been left out of equation (12).

Among all the elemental metals, excluding the rare-earths, Sc has the largest electronic specific heat constant γ, followed by Y and Pd [40]. The reported experimental values at normal pressure are 10.9–10.33 mJ mol^{-1} K^{-2} [25, 37, 40–43]. Considering the latest and the most conservative value of $\gamma = 10.33$ mJ mol^{-1} K^{-2} [25, 41], we get $N^*(0) = 2.2$ states/(eV atom spin). With the calculated value of 1.067 states/(eV atom spin), we get $\lambda_{\mathrm{eff}} = 1.063$. The calculated value of $\lambda_{\mathrm{ph}} = 0.639$ then yields $\lambda_{\mathrm{sf}} = 0.422$. Effects of spin fluctuations on T_c can be incorporated by a simple rescaling of λ_{ph} and the Coulomb pseudopotential μ^*: $\lambda_{\mathrm{ph}} \rightarrow \lambda_{\mathrm{ph}}/(1 + \lambda_{\mathrm{sf}})$, $\mu^* \rightarrow (\mu^* + \lambda_{\mathrm{sf}})/(1 + \lambda_{\mathrm{sf}})$ [44]. An extension of the McMillan formula [13] that is often used to incorporate the spin fluctuation effects is

$$T_c = \frac{\omega_{\ln}^{\mathrm{ph}}}{1.2} \exp\left\{ -\frac{1.04(1 + \lambda_{\mathrm{ph}} + \lambda_{\mathrm{sf}})}{\lambda_{\mathrm{ph}} - \lambda_{\mathrm{sf}} - \mu^*[1 + 0.62(\lambda_{\mathrm{ph}} + \lambda_{\mathrm{sf}})]} \right\}. \qquad (14)$$

This formula is meaningful as long as λ_{sf} is sufficiently less than λ_{ph}, so that the denominator in the argument of the exponential in equation (14) stays positive and not close to zero. For the above values of λ_{ph}, λ_{sf} and the Coulomb

pseudopotential $\mu^* = 0.16$ (see table 3), this condition breaks down. In fact, for comparable values of λ_{ph} and λ_{sf}, the Kernel of the Eliashberg equation (equation (2)) $W_-(n - n')$, given by equation (4), becomes negative, allowing no solution for T_c. It should be emphasized that the McMillan-type formulas in the presence of spin fluctuations are good for rough ball-park estimates of T_c only.

Note that our calculated value of $\lambda_{ph} = 0.639$ for normal pressure hcp Sc is significantly higher than the value $\lambda_{ph} = 0.3$ that has been suggested by Knapp and Jones [45], based on a comparison of the high and low temperature electronic specific heats. A value of $\lambda_{ph} = 0.3$ would suggest $\lambda_{sf} = 0.76$, more than twice larger than λ_{ph}. Our results suggest that $\lambda_{sf} < \lambda_{ph}$, but their values are close. This leads to the possibility that if spin fluctuations can be suppressed via application of pressure, superconductivity can indeed appear.

Based on the analysis of high and low temperature specific heats, Knapp and Jones [45] also suggested that for Pd $\lambda_{ph} = 0.7$. The electronic specific heat constant γ for Pd is only slightly lower than that in hcp Sc [40, 45], lying between 10.0 and 9.2mJ mol^{-1} K^{-2}. The calculated bare band density of states $N(0)$ for fcc Pd is about 1.3 states/(eV atom spin), giving λ_{eff} in the range 0.66 and 0.5. An analysis by Savrasov and Savrasov [8] puts the value at 0.69. The value $\lambda_{ph} = 0.7$ suggested by Knapp and Jones would leave no room for spin fluctuation effects in Pd, and would render Pd superconducting. The FP-LMTO linear response calculation for fcc Pd by Savrasov and Savrasov [8] yields $\lambda_{ph} = 0.35$, giving λ_{sf} in the range 0.3–0.15. These values of λ_{ph} and λ_{sf} can adequately explain the nonexistence of superconductivity in fcc Pd. We have repeated the linear response calculation for fcc Pd and obtain a value of $\lambda_{ph} = 0.37$, in close agreement with the result of Savrasov and Savrasov [8]. Note that the calculation by Pinski and Butler [46] based on the RMT approximation yields $\lambda_{ph} = 0.41$ for fcc Pd, in reasonable agreement with the FP-LMTO linear response results. To summarize, our linear response calculations and electronic specific heat analysis show that in both hcp Sc and fcc Pd the values of electron–phonon and electron–paramagnon coupling constants are comparable, with the latter being slightly lower. This is qualitatively different from the previous results of Knapp and Jones [45], which would suggest that in Sc λ_{ph} is significantly lower than λ_{sf}, and vice versa for fcc Pd. Note that according to our results both λ_{ph} and λ_{sf} are larger in hcp Sc than the corresponding quantities in fcc Pd.

While the nature of spin fluctuations in fcc Pd is accepted to be ferromagnetic, that in hcp Sc could be antiferromagnetic. The dynamic susceptibility $\chi(q, \omega)$ in Pd has a peak at $q = 0$, whereas $\chi(q, \omega)$ in hcp Sc is expected to have a peak at some finite wavevector Q. First-principles calculation of $\chi(q)$ including spin–orbit coupling and all other relativistic effects by Thakor *et al* [47] yields a peak at the wavevector $\mathbf{q} = (0, 0, 0.57\pi/c)$, consistent with a Fermi surface nesting vector. Earlier calculations produce a peak along the same direction but at different values [48, 49] of q. Capellmann [35] has discussed the effect of incipient antiferromagnetism in Sc and shown that the antiferromagnetic spin fluctuations should lead to a repulsive electron–electron interaction, resulting in

suppression of superconductivity. The modified McMillan formula (equation (14)) has been used to estimate T_c for both ferromagnetic and antiferromagnetic spin fluctuations [12, 13].

5.2. Superconductivity in hcp Sc at high pressure immediately before the transition to the Sc-II phase

Our linear response calculation yields a high value $\lambda_{ph} \sim 1.0$ of the electron–phonon coupling constant at the high pressure hcp phase prior to the transition to the complex Sc-II structure. It is natural to ask whether spin fluctuations should be able to suppress superconductivity despite such strong electron–phonon coupling. Since specific heat data are not available for such high pressures, a reliable estimate of λ_{sf} is difficult. However, a reasonable step might be to scale the ambient pressure λ_{sf} according to the density of states $N(0)$ at high pressure shown in table 1. This gives $\lambda_{sf} = 0.346$ for the smallest volume or the highest pressure calculation. With $\lambda_{ph} = 1.0$, $\lambda_{sf} = 0.346$, $\mu^* = 0.166$, and $\omega_{ln} = 177.7$ K, as shown in table 3, and using equation (14), we get $T_c = 0.14$ K. As pointed out earlier, at comparable values of λ_{ph} and λ_{sf}, equation (14) may not be reliable, and one needs to solve the Eliashberg equation. However, our estimate of $T_c = 0.14$ K indicates that there is a possibility of hcp Sc turning superconducting just before the onset of the high pressure Sc-II phase. This is indeed what has been reported by Wittig *et al* [2]. Note that such a conclusion would not be tenable for smaller values of λ_{ph}, as the results of Knapp and Jones [45] would suggest.

The use of the energy-optimized c/a ratio at higher than ambient pressures may change the calculated values of λ_{ph} somewhat, but such small changes are not expected to influence our results qualitatively and will not affect the nature of the conclusions.

5.3. Superconductivity in the Sc-II phase

Spin fluctuations are expected to be significantly reduced in the Sc-II phase. According to the calculations of Ormeci *et al* [22], the density of states at the Fermi level $N(0)$ in the Sc-II structure should be about half the value in the ambient pressure hcp Sc. This suggests that λ_{sf} should be reduced to a value of 0.2 or less. Reasonable choices of ω_{ln} in the Sc-II phase at pressures ~ 30 GPa (see table 3) and μ^* should be 210.0 K and 0.166, respectively. A value of $\lambda_{ph} = 0.95$ in equation (14) would yield a $T_c = 1.4$ K. Reducing the value of λ_{sf} to 0.1 would result in a T_c of 4.5 K. These numbers suggest that superconductivity in the Sc-II phase can be explained based on the quantities calculated for the high pressure hcp Sc and reasonable estimates of the reduction in the spin fluctuation effects that is expected as a result of the change in the density of states. Note that phonon softening causes λ_{ph} to increase in the hcp phase immediately before the transition to the Sc-II structure. At the start of the Sc-II phase the value of λ_{ph} should be somewhat less than the value 1.033 shown in table 3, hence the choice 0.95. It should be noted that although the density of states $N(0)$ decreases with increasing pressure, there is a rapid increase in the electron–phonon matrix element $\langle I^2 \rangle$ with decreasing volume (see table 3). A high value of λ_{ph} in the

Sc-II phase is thus possible despite the reduced value of $N(0)$. Chances are that at the start of the Sc-II phase both λ_{ph} and λ_{sf} are somewhat less than the values suggested here.

6. Comparison between hcp Sc and hcp Fe

The bulk moduli of all transition metals are known to increase (at least initially) as a function of band filling[2], and the bulk moduli of the late transition metals are in general higher than those of the early ones. The bulk modulus of Fe is thus expected to be larger than that of Sc, a consequence of Fe having more d-electrons. The calculations of Bose *et al* [12] for the hcp phase of Fe show values in the range of 300 GPa to 970 GPa, corresponding to volumes per atom for which the calculated T_c is above zero (the theoretical superconducting phase). These values are 4–5 times higher than the bulk modulus values of Sc shown in table 1. Accordingly, the average phonon frequency in hcp Fe is about four times higher than in Sc. Because of a much larger number of d-electrons in hcp Fe (6.5 on average) than Sc (1.6 on average), the electron–phonon matrix element $\langle I^2 \rangle$ in Fe is also much larger. As a result, despite the lower value of $N(0)$, the Hopfield parameter $\eta = N(0)\langle I^2 \rangle$ in hcp Fe turns out to be more than double that in Sc (compare table 3 with table II of [12]). However, the dominating effect turns out to be the lower phonon frequencies in Sc, leading to higher values of λ_{ph}.

Spin fluctuations, most probably of an antiferromagnetic nature [12, 13], are believed to be present in the high pressure hcp phase of Fe. Because the density of states $N(0)$ in hcp Fe is about half that in hcp Sc, spin fluctuations in hcp Fe should be much weaker. There is no specific heat data available for hcp Fe, the stable phase of Fe at pressures of $\sim$10 GPa and higher. As a result, an experimental estimate of λ_{sf} in hcp Fe is not available. Some theoretical estimates were provided in [12, 13].

For a crude estimate of the ratio between the values of λ_{ph} for hcp Fe and Sc, we can assume the Hopfield parameter η to be simply proportional to the fractional d-DOS, $N_d(0)/N(0)$. For an estimate of $m\langle \omega^2 \rangle$, we can use the result proposed by Moruzzi *et al* [50], relating the Debye temperature Θ_D to the bulk modulus, atomic mass and the average Wigner–Seitz radius:

$$\Theta_D = 41.63\sqrt{\frac{s_0 B}{m}}, \qquad (15)$$

where s_0 is the average Wigner–Seitz radius in au and B is the bulk modulus in kbar. This result suggests that $m\langle \omega^2 \rangle \propto s_0 B$. Using B values from table 1 and table I of [12], the DOS values from table 2, s_0 computed from $a = 4.6$ au, $c/a = \sqrt{8/3}$ for Fe and $a = 6.255$ au, $c/a = 1.592$ for Sc, we get $\lambda_{Fe}/\lambda_{Sc} = 0.45$. This compares favorably with the value 0.66, according to the computed linear response values (table III and table II of [12]). We have used $N_d(0) = 34.55$ states/(Ryd cell) and $N(0) = 40.79$ states/(Ryd cell) (table I of [12]) for Fe. The proportionality of η to fractional d-DOS, $N_d(0)/N(0)$, can be

somewhat justified on the basis of the RMT result of Gaspari and Gyorffy [30]:

$$\eta = 2N(0)\sum_l (l+1)M_{l,l+1}^2 \frac{f_l}{2l+1}\frac{f_{l+1}}{2l+3}, \qquad (16)$$

where $N(0)$ is the Fermi level DOS per atom per spin and f_l is a relative partial state density,

$$f_l = \frac{N_l(0)}{N(0)}. \qquad (17)$$

$M_{l,l+1}$ is the electron–phonon matrix element obtained from the gradient of the potential and the radial solutions R_l and R_{l+1} of the Schrödinger equation evaluated at the Fermi energy. Neglecting the matrix elements and all partial DOSs other than $N_d(0)$ amounts to the result $\eta \propto N_d(0)/N(0)$. Of course, this provides a very crude estimate and can only be relied on in deciding whether λ for one material is greater or lower than for the other and no quantitative reliability can be guaranteed. In fact, in getting the estimate $\lambda_{ph,Fe}/\lambda_{ph,Sc} = 0.45$ we have ignored the possible differences in the p- and f-DOSs of the two solids. Consideration of these differences would lead to an inferior quantitative agreement. Also, the ratio $m\langle \omega^2 \rangle$ for Fe to Sc for the volumes considered is 2.35 according to equation (15), while the value from the linear response calculation is 3.5.

7. Summary

FP-LMTO linear response calculations for the hcp phase of Sc, based on a fixed c/a ratio of 1.592, shows a monotonic increase in electron–phonon coupling with pressure. Calculated phonon frequencies for the equilibrium lattice parameter are 6–10% lower than those obtained via INS experiments [24]. The agreement can perhaps be improved with calculations done on a finer wavevector mesh. The estimated pressure, based on the linear response results, for the instability to appear is 23–30 GPa. This pressure range, which can certainly be narrowed with additional calculations, agrees with the experimental observations. The Γ-point E_{2g} frequency shows a modest increase with pressure, in qualitative agreement with the Raman work by Olijnyk *et al* [26]. Energy-optimized choice of the c/a ratio for each volume per atom may lead to a better agreement.

The electron–phonon coupling constant λ_{ph} is found to increase steadily with pressure in the hcp phase, until the pressure reaches a value where the hcp phase becomes unstable. An estimate of the electron-paramagnon coupling constant based on the measured temperature coefficient of the electronic specific heat, calculated band density of states and λ_{ph} suggests that the spin fluctuations at normal pressure should be strong enough to suppress superconductivity completely. At the highest pressures where the hcp phase is still stable, the increase in λ_{ph} and a decrease in λ_{sf} in proportion to the calculated band density of states suggest the possibility of a very low T_c superconductivity, as noted by Wittig *et al* [2]. A comparison of the band densities of states in the hcp and the Sc-II phases shows that the spin

---

[2] See, for example, page 148, figure 25 of [20].

fluctuation effects in the Sc-II phase should be reduced by a factor of two or more. It is argued that this suppression of spin fluctuation combined with electron–phonon coupling constants of a magnitude similar to that calculated for the high pressure hcp phase can indeed account for the observed superconductivity in the Sc-II phase.

Acknowledgments

References

[1] Hamlin J J and Schilling J S 2007 *Phys. Rev.* B **76** 012505
   See also Hamlin J J and Schilling J S 2007 *Preprint* cond-mat/0703730v1
[2] Wittig J, Probst C, Schmidt F A and Gschneidner K A Jr 1979 *Phys. Rev. Lett.* **42** 469
[3] Fujihisa H *et al* 2005 *Phys. Rev.* B **72** 132103
[4] Akahama Y, Fujihisa H and Kawamura H 2005 *Phys. Rev. Lett.* **94** 195503
[5] McMahon M I, Lundegaard L F, Hejny C, Falconi S and Nelmes R J 2006 *Phys. Rev.* B **73** 134102
[6] Savrasov S Yu and Savrasov D Yu 1992 *Phys. Rev.* B **46** 12181
[7] Savrasov S Y 1996 *Phys. Rev.* B **54** 16470
[8] Savrasov S Y and Savrasov D Y 1996 *Phys. Rev.* B **54** 16487
[9] Kittel C 1996 *Introduction to Solid State Physics* 7th edn (New York: Wiley) p 23
[10] Shimizu K, Kimura T, Furomoto S, Takeda K, Kontani K, Onuki Y and Amaya K 2001 *Nature* **412** 316
   see also Saxena S S and Littlewood P B 2001 *Nature* **412** 290
[11] Jaccard D, Holmes A T, Behr G, Inada Y and Onuki Y 2002 *Phys. Lett.* A **299** 282–6 (*Preprint* cond-mat/0205557)
[12] Bose S K, Dolgov O V, Kortus J, Jepsen O and Andersen O K 2003 *Phys. Rev.* B **67** 214518
[13] Mazin I I, Papaconstantopoulos D A and Mehl M J 2002 *Phys. Rev.* B **65** 100511(R)
[14] Perdew J P, Chevary J A, Vosko S H, Jackson K A, Pederson M R, Singh D J and Fiolhais C 1992 *Phys. Rev.* B **46** 6671
[15] Blöchl P E *et al* 1994 *Phys. Rev.* B **49** 16223
[16] Birch F 1952 *J. Geophys. Res.* **457** 227
[17] Murnaghan F D 1944 *Proc. Natl Acad. Sci. USA* **30** 244
[18] Pettifor D G 1977 *J. Phys. F: Met. Phys.* **7** 623
[19] Duthie J C and Pettifor D G 1977 *Phys. Rev. Lett.* **38** 564
[20] Andersen O K, Jepsen O and Glötzel D 1985 *Highlights of Condensed Matter Theory* ed F Bassani *et al* (Amsterdam: North-Holland) p 59
[21] Perdew J P and Wang Y 1992 *Phys. Rev.* B **45** 13244
[22] Ormeci A, Koepernik K and Rosner H 2006 *Phys. Rev.* B **74** 104119
[23] Koepernik K and Eschrig H 1999 *Phys. Rev.* B **59** 1743
[24] Wakabayashi N, Sinha S K and Spedding F H 1971 *Phys. Rev.* B **4** 2398
   Dederichs P H, Schober H and Sellmyer D J (ed) 1981 *Metals: Phonon and Electron States and Fermi Surfaces* (*Landöldt-Bernstein New Series* 111/13a) (Berlin: Springer) (series ed K-H Hellwege and J L Olsen)
[25] Pleschiutschnig J, Blaschko O and Reichardt W 1991 *Phys. Rev.* B **44** 6794
[26] Olijnyk H, Nakamo S, Jephcoat A P and Takemura K 2006 *J. Phys.: Condens. Matter* **18** 10971
[27] Olijnyk H 1994 *High Pressure Res.* **13** 99
[28] Olijnyk H 2005 *J. Phys.: Condens. Matter* **17** 43
[29] Allen P B and Mitrović B 1982 *Solid State Physics* vol 37, ed H Ehrenreich, F Seitz and D Turnbull (New York: Academic) p 1
[30] Gaspari G D and Gyorffy B L 1972 *Phys. Rev. Lett.* **28** 801
[31] Glötzel D, Rainer D and Schober H R 1979 *Z. Phys.* B **35** 317
[32] Skriver H L and Mertig I 1985 *Phys. Rev.* B **32** 4431
   Skriver H L and Mertig I 1993 *Phys. Rev.* B **32** 5325
[33] Bose S K, Kato T and Jepsen O 2005 *Phys. Rev.* B **72** 184509
[34] Berk N F and Schrieffer J R 1966 *Phys. Rev. Lett.* **17** 433
[35] Capellmann H 1970 *J. Low Temp. Phys.* **3** 189
[36] Das S G 1976 *Phys. Rev.* B **13** 3978
[37] Jensen M A and Maita J P 1966 *Phys. Rev.* **149** 409
[38] MacDonald A H, Liu K L and Vosko S H 1977 *Phys. Rev.* B **16** 777
[39] Janak J F 1977 *Phys. Rev.* B **16** 255
[40] See table XIII and figure 18 of Gschneidner K A Jr 1964 *Solid State Physics* vol 16, ed F Seitz and D Turnbull (New York: Academic) pp 275–426
[41] Tsang T-W E, Gschneidner K A Jr, Schmidt F A and Thome D K 1985 *Phys. Rev.* B **31** 235
[42] Flotow H E and Osborne D W 1967 *Phys. Rev.* **160** 467
[43] Swenson C A 1996 *Phys. Rev.* B **53** 3669
[44] Daams J M, Mitrović B and Carbotte J P 1981 *Phys. Rev. Lett.* **46** 65
[45] Knapp G S and Jones R W 1972 *Phys. Rev.* B **6** 1761
[46] Pinski F J and Butler W H 1979 *Phys. Rev.* B **19** 6010
[47] Thakor V, Staunton J B, Poulter J, Ostanin S, Ginatempo B and Bruno E 2003 *Phys. Rev.* B **68** 134412
[48] Rath J and Freeman A J 1975 *Phys. Rev.* B **11** 2109
[49] Liu S, Gupta R P and Sinha S K 1971 *Phys. Rev.* B **4** 1100
[50] Moruzzi V L, Janak J F and Schwartz K 1988 *Phys. Rev.* B **37** 790